Supplementary Materials for

Marine heatwaves deeply alter marine food web structure and function

S1: MHW loss rate algorithm computation

- MHW characterisation and detection

To characterise MHW in each ocean spatial cell, we analysed daily SST observations from the NOAA's AVHRR data (Reynolds et al., 2007; https://www.ncei.noaa.gov/access/metadata/landing-page/bin/iso?id=gov.noaa.ncdc:C00680). We defined MHW as a discrete prolonged anomalously warm water event when the daily SSTs exceed an extreme temperature threshold value for at least five consecutive days (A. J. Hobday et al., 2016). The extreme temperature threshold value was calculated for each 1° latitude x 1° longitude spatial cell as the 90th percentile of daily SST from the 30-year historical time series from January 1982 to December 2011. We did not calculate threshold values by season; thus, MHW events were identified by a single threshold across the year. As a result, we detected MHWs mostly occurring during the year's warmest months (see figure S1a for schematic explanation). This approach to identifying the MHW threshold represents biological extreme temperature in the local (spatial cell) context. It is appropriate to assess the direct mortality associated with MHWs (Oliver et al., 2021). We determined a reference average sea surface temperature (SST average) for each spatial cell by analysing data from the 1st of January 1982 to the 31st of December 2011. Utilising this reference average SST, we classified each spatial cell into 'thermal classes,' with each class representing a 1°C increment of the reference SST average ranging from -1°C to 29°C (refer to Figure S1b). We used the R package heatwaveR described at https://robwschlegel.github.io/heatwaveR/ to compute MHWs characteristics in each spatial cell from January 1982 to December 2021. Thus, we finally obtained MHW characteristics for each 1° per 1° of longitude and latitude ocean cell up to December 2021. The considered MHW characteristics are the threshold value defining MHWs, MHW's duration (in days), category and intensity (mean SST anomaly) and declaration of MHW days over the SST time series.

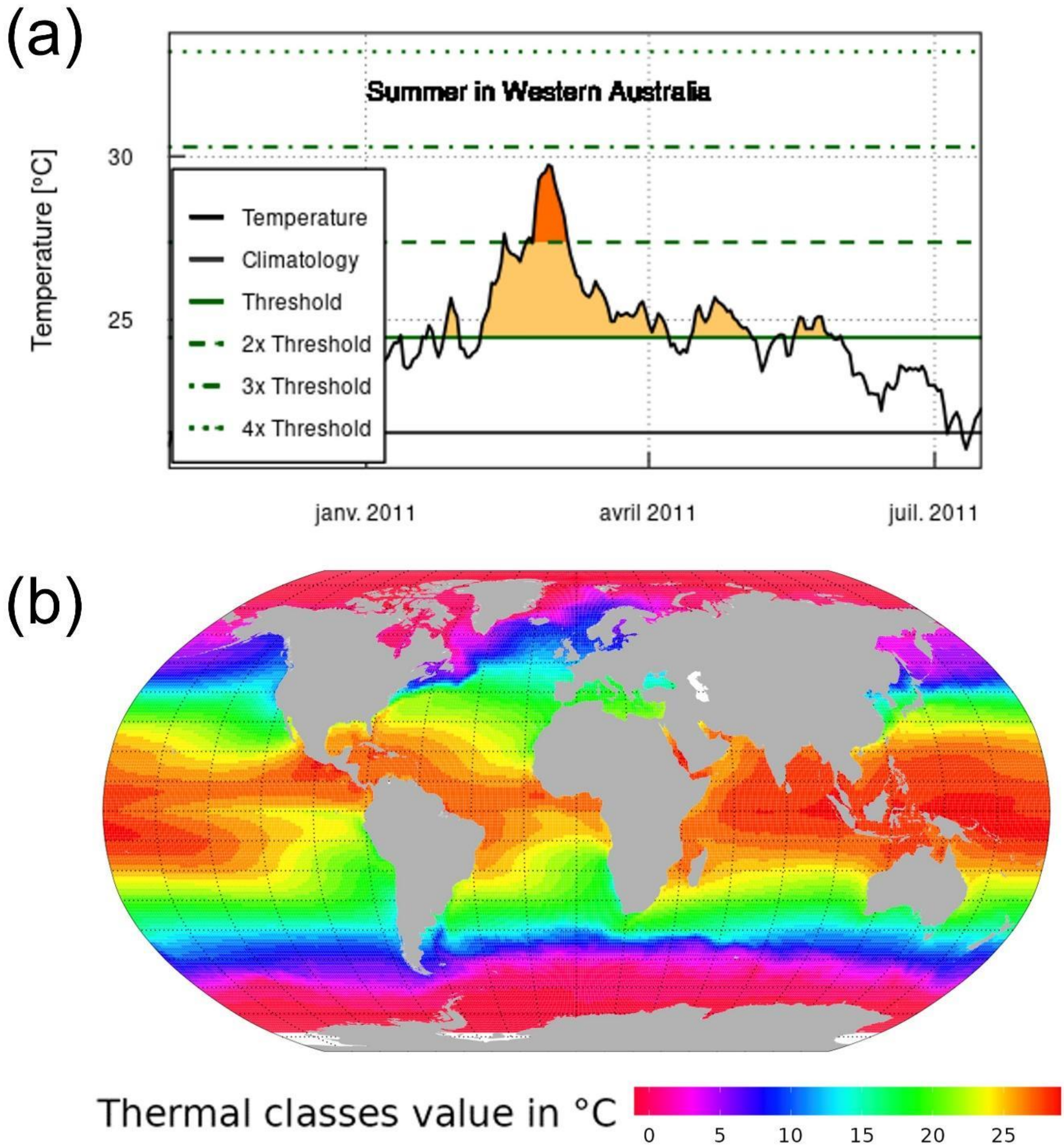

Figure S1: Marine heatwave detection method and reference average SST of each ocean cell. (a) Schematic explanation of MHWs detection for a spatial cell. The solid horizontal green and black lines represented the extreme threshold value and the reference temperature, respectively. (b) A map of thermal classes of 1o C intervals from -1 to 29°C categorised based on the reference temperature at each spatial cell over the period from 1st January 1982 to 31st December 2011.

- Estimation of species distribution and associated thermal niche

We developed an algorithm depending on the MHWs' characteristics to express the loss rate of trophic transfers associated with MHW. First, we identified a list of marine species with their occurrence records (3242 bivalves, 500 cephalopods species, 3116 crabs species, and 12782 fish species) gathered from the publicly accessible databases: OBIS (www.iobis.org), the Intergovernmental Oceanographic Commission (ioc-unesco.org), GBIF (www.gbif.org), Fishbase (www.fishbase.org), and the International Union for the Conservation of Nature (http://www.iucnredlist.org/technical-documents/spatial-data). We then cleaned the data by removing duplicate entries, terrestrial occurrences, and occurrences outside the known species habitat from the aggregated species occurrence dataset (Froese & Pauly, 2018). Additionally, we excluded zooplankton from the algorithm development due to limited evidence of direct mortality induced by Marine Heatwaves (MHWs), with observed responses mainly manifesting as range shifts and alterations in community structure (Arimitsu et al., 2021; Suryan et al., 2021; Winans et al., 2023). Marine mammals and seabirds were also omitted from algorithm development, as their mortality linked to MHWs primarily stems from secondary effects such as diminished quality and quantity of food supply (Cavole et al., 2016; Piatt et al., 2020) rather than direct heat stress impact. Subsequently, the data were rasterised into a grid covering the global oceans (1° longitude by 1° latitude), denoting the historical presence of each species. Species with occurrence records in fewer than 30 cells were excluded from further analysis (Hernandez et al., 2006).

In a second step, we utilised an ensemble species distribution modelling approach (Asch et al., 2018; Reygondeau, 2019) at a 1° grid scale. Four environmental niche models (ENMs) were applied: Bioclim, Boosted Regression Trees models (Thuiller et al., 2009), Maxent (Phillips et al., 2006), and the Non-Parametric Probabilistic Ecological Niche model (Beaugrand et al., 2011), using global climatology satellite data (AVHRR). Model accuracy was assessed using the area under the curve (AUC) analysis of the receiver operating characteristic (ROC), discarding models with AUC below 0.5 (Sing et al., 2005). The evaluation employed the pROC package in R (Robin et al., 2011). We then calculated the average

Habitat Suitability Index (HSI) weighted by the AUC values of each ENM for each spatial cell and species. An HSI threshold for each species was estimated using their prevalence. Spatial cells with HSI below the threshold were deemed non-viable habitats.

Species' predicted thermal niches were quantified from spatial distributions using averaged satellite sea surface temperature (SST) data (AVHRR) from 1982 to 2011. The average SST from 1982 to 2011 was recorded for each spatial cell above the HSI threshold. We then characterised the predicted thermal niche (histogram of all the average values of SST), and more specifically, the upper-temperature threshold, for each species from the 95th percentile of the SST records where they were predicted to occur.

- Additional loss rate associated with MHW

For each spatial cell belonging to each thermal class, we calculated the percentage of species in each trophic class exposed to thermal stress induced by MHWs intensity above their estimated temperature threshold (95th percentile of their thermal niche). Matching MHW intensity in each spatial cell from 1981 to 2021 with species' temperature thresholds, we determined the percentage of species exposed to temperatures exceeding their thresholds. Thermal stress of a species was assumed dependent on MHW category (1 to 4, based on SST anomaly) and species' trophic level (<2.5, 2.5-3.0, 3.0-3.5, 3.5-4.0, 4.0-4.5, 4.5-5.0, >5.0), estimated from FishBase and SeaLifeBase.

To obtain a continuous representation of the percentage of species undergoing a thermal stress as the intensity of MHW increases, we decided to transform the discrete MHW categorisation (A. Hobday et al., 2018) to a continuous MHW intensity index as follows:

$$MHW_{cat,i} = \frac{MHW\ mean\ anomaly,i}{cat1\ associated\ anomaly,i} \quad \text{(Eq. S1)}$$

MHW mean anomaly was calculated as the difference between the MHW mean SST anomaly and the reference temperature of each thermal class (i), and “cat1 associated anomaly” is the mean threshold value used to identify category 1 MHWs in each spatial cell.

We fit the estimated percentage of species undergoing thermal stress with the MHW intensity index and species' trophic class to a nonlinear function. A Gompertz function was selected after preliminary tests because it is better fitted to data than logistic or other mathematical functions with similar shapes. The Gompertz function is expressed as:

$$Percentage\ of\ species\ undergoing\ a\ thermal\ stress = exp^{-exp^{b\_tl_i \cdot (MHW_{cat,i} - lt50\_tl_i)}} \quad \text{(Eq. S2);}$$

We estimated the parameters b_tl_i, $lt50\_tl_i$, and $MHW_{cat,i}$ for each thermal class i. The parameters b_tl_i and $lt50\_tl_i$ correspond to the slope of the function and the index of marine heatwave intensity ($MHW_{cat,i}$) at which 50% of the species are undergoing thermal stress, respectively.

For each thermal class i, parameters b_tl_i and $lt50\_tl_i$ were expressed as (figure S2):

$b\_tl_i = -1.4511 - e^{0.4223 \cdot (i - 22.4926)}$ (Eq. S3) and

$lt50\_tl_i = 3.29 - 0.485 \cdot i + 0.0306 \cdot i^2 - 0.000608 \cdot i^3$ when trophic level <2.5 and

$lt50\_tl_i = 3.55 - 0.271 \cdot i + 0.014 \cdot i^2 - 0.000304 \cdot i^3$ when trophic level >=2.5. (Eq. S4)

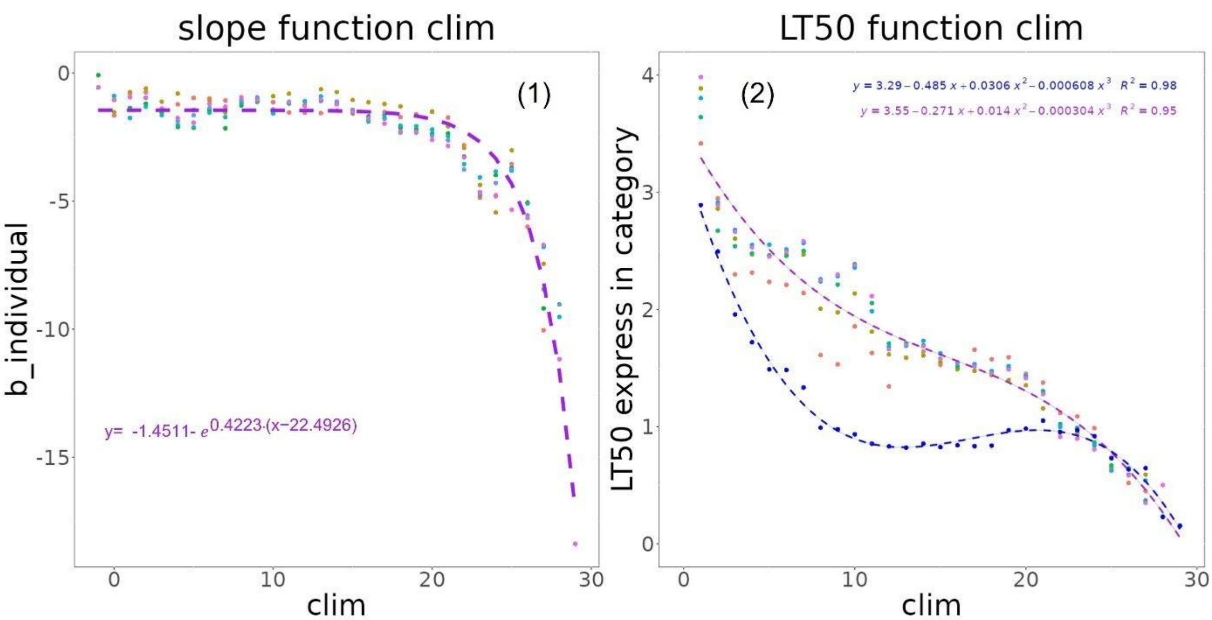

Figure S2: coefficient of each reference temperature individual thermal stress algorithm model. With (1) corresponding to the Gompertz slope at the inflexion point coefficient (b) and (2) the MHW category that causes 50% of species to undergo thermal stress (lt50) with blue and other colours corresponding to the trophic levels below 2.5 and above 2.5, respectively.

Finally, to move from the thermally stressed stage to the loss rate (η_i), we assumed that species were continuously challenged by MHW increased intensity (Figure S3 for schematic differences) expressed as.

$$\eta_i = exp^{-exp^{b_i \cdot \alpha \cdot \left(MHW_{cat,i} - \frac{lt50_i}{\alpha}\right)}} \cdot \beta \quad \text{(Eq. S5)}$$

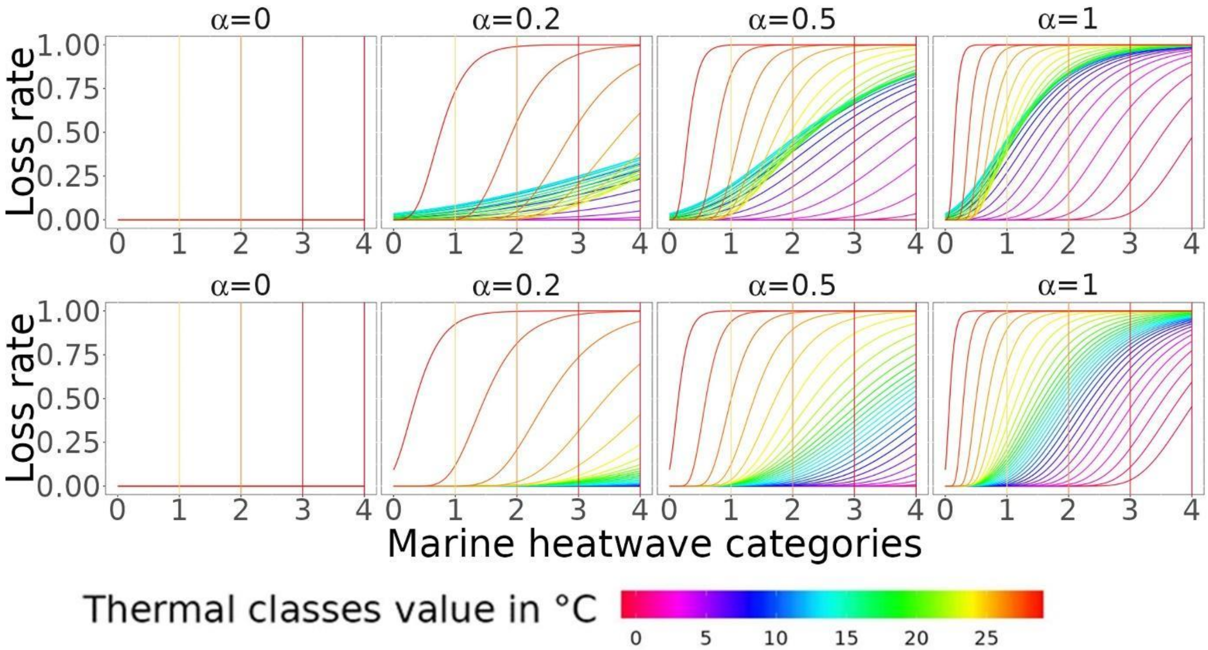

Figure S3: loss rate associated with MHWs occurrences. With the ecological hypothesis that MHW increases in intensity/category continuously challenge the aggregated response across species. On the plots, b is equal to 1. The top bottom and bottom rows correspond to the loss rate of trophic level <2.5 and trophic level>=2.5, respectively.

We explored the sensitivity of the results to species' acclimation capacity to MHW conditions by assuming that acclimation reduces the mortality rate due to species' exposure to thermal stress. We tested four acclimation capacity settings represented by the values of the coefficient α. These settings are full acclimation (α = 0; no mortality due to thermal stress), partial acclimation (α = 0.2, 0.5; 20%, and 50% of the species die because of thermal stress, respectively) and no acclimation (α =1; all species die when they are under thermal stress). We also related the loss rate to the MHW duration over the fortnight by assuming that the duration increases the mortality rate. The duration of MHW is represented by β and ranges from $\beta=0$; no MHW to $\beta=1$; MHW lasting 15 days of the fortnight (see section 2.3.2 for β computation).

S2: Study area.

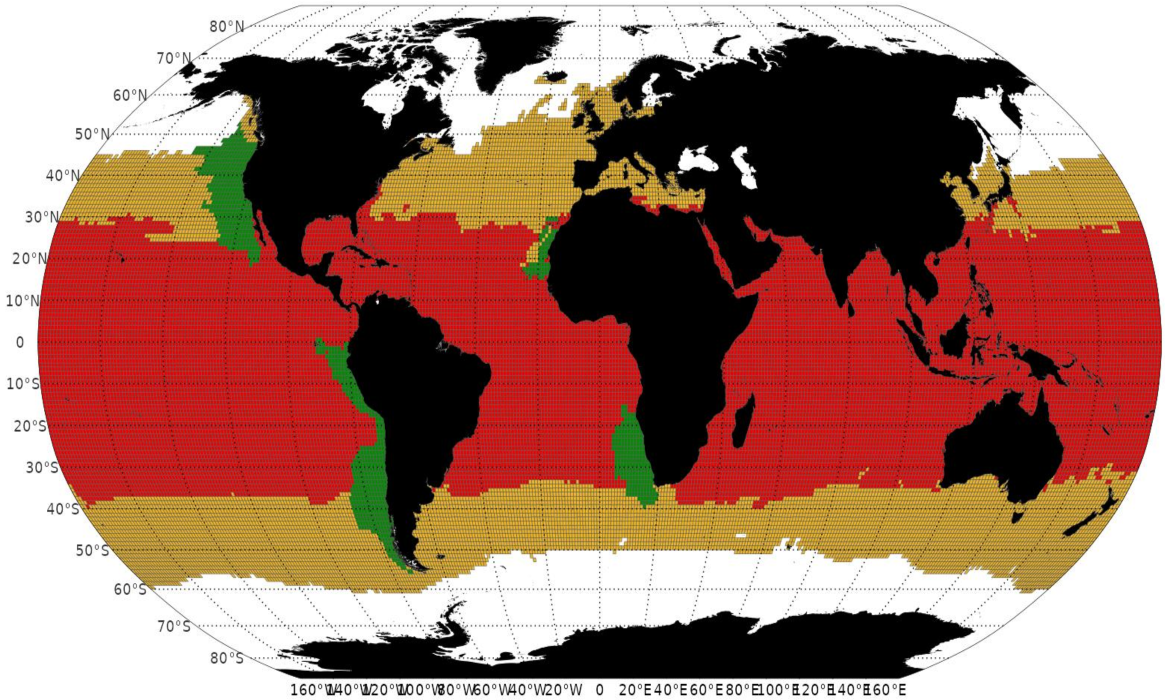

Figure S4: Map of where EcoTroph-Dyn was applied and the associated biome types. The colours refer to the biome types: temperate (orange), tropical (red) and upwelling (green).

S3: Time series decomposition

To create scenarios without MHWs SST time series, we decomposed the daily SST time series (Y_t) of each ocean spatial cell using a Census X-11 procedure (Vantrepotte and Mélin, 2011, Shiskin et al 1967,Pezulli et al 2005). With this method, the time series can be decomposed as:

$$Y_t = T_t + S_t + H_t$$

With Y_t the daily SST of day t, T_t the underlying long-term direction component, S_t the seasonal component (repetitive pattern over time), and H_t an irregular component, which is the unexplained variation of the time series that is not attributed to trend or seasonality.

The T_t underlying long-term direction is obtained from the annual-centered running average of the initial series Y_t. The S_t the seasonal component is then computed by applying a seasonal running mean to the trend-adjusted series (Y_t–T_t) to derive seasonal coefficients avoiding any confusion with the inter-annual (trend) signal. after revised estimates of these two components (Vantrepotte and Mélin, 2011, Pezulli et al 2005), the residual component is computed as

$H_t = Y_t - S_t - T_t$.

We applied the following procedure to create a daily SST time series for the scenarios without MHWs:

When the daily Y_t value was declared as an MHW day and $Y_t$was above the threshold ($T_t + S_t$), we re-assigned the daily SST value (Y_t) to the value of the threshold ($T_t + S_t$). For all the others situations (MHW day with Y_t below the threshold ($T_t + S_t$) or that the day was not an MHW day), we let the daily SST value Y_t assigned to its original value (figure S5).

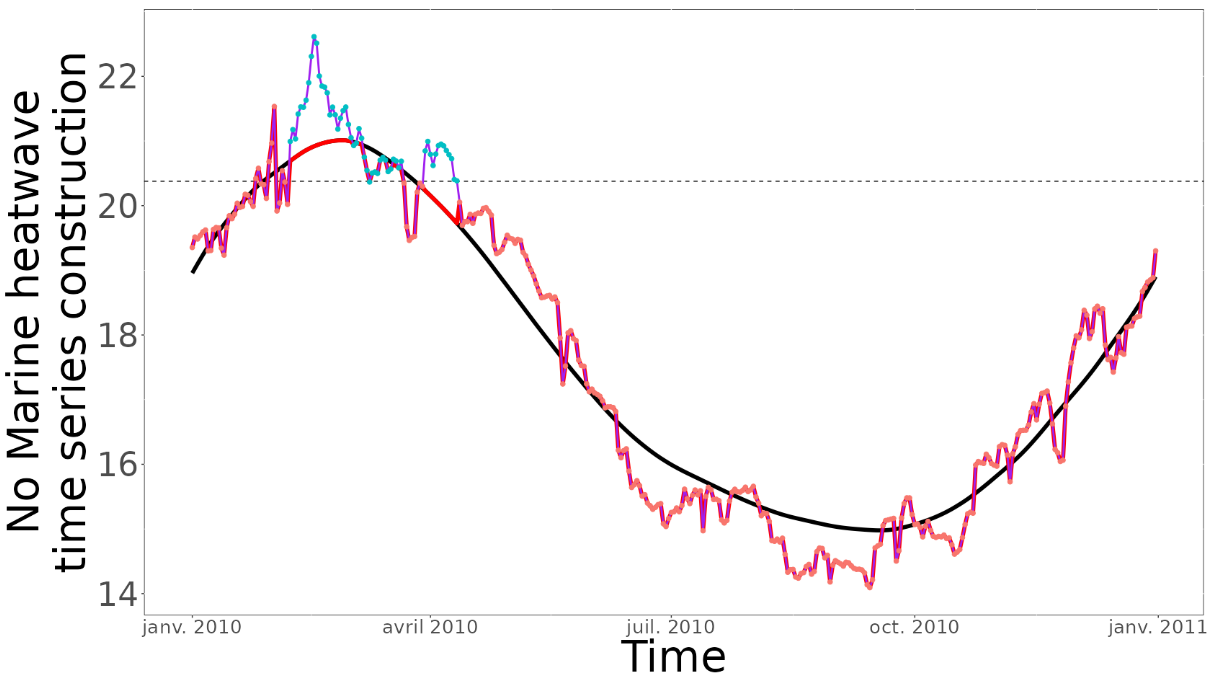

Figure S5: Illustration of the removal of MHWs from the time series. With blue and red points correspond to MHW days and non-MHW days, respectively. The original time series of SST, represented by Y_t, is shown as a thin purple line. The time series of SST with MHWs removed is depicted by a thick red line. The combination of the long-term linear trend and the seasonal component denoted as $T_t + S_t$, is illustrated with a thick black line. Additionally, the dotted grey line represents the fixed threshold value used for detecting MHWs in the specific ocean cell chosen for the illustration.

S4: ‘Burn in’ period applied to EcoTroph-Dyn model.

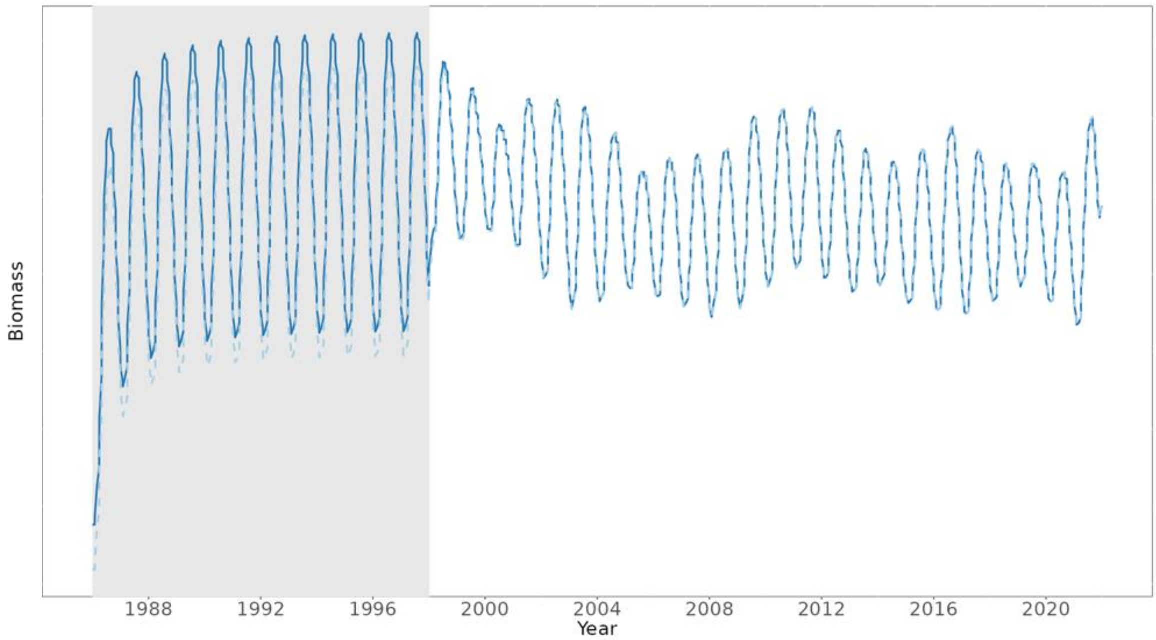

Figure S6: Illustration of the removal of MHWs from the time series. With initialisation period 1998_2021 and 1998_2006 corresponding to the darker blue solid line and lighter blue dashed line, respectively. The vertical grey shaded area indicates the 12 years of initialisation period. Afterward the hindcast analysis begins. Tests demonstrated no statistically significant differences, indicating that EcoTroph-Dyn simulations were not dependent of the initialization period onward (t.test p_value=0.6118).

S5: Yearly simulation masked the effects of the short-term impacts of MHWs on the long-term changes in consumer biomass

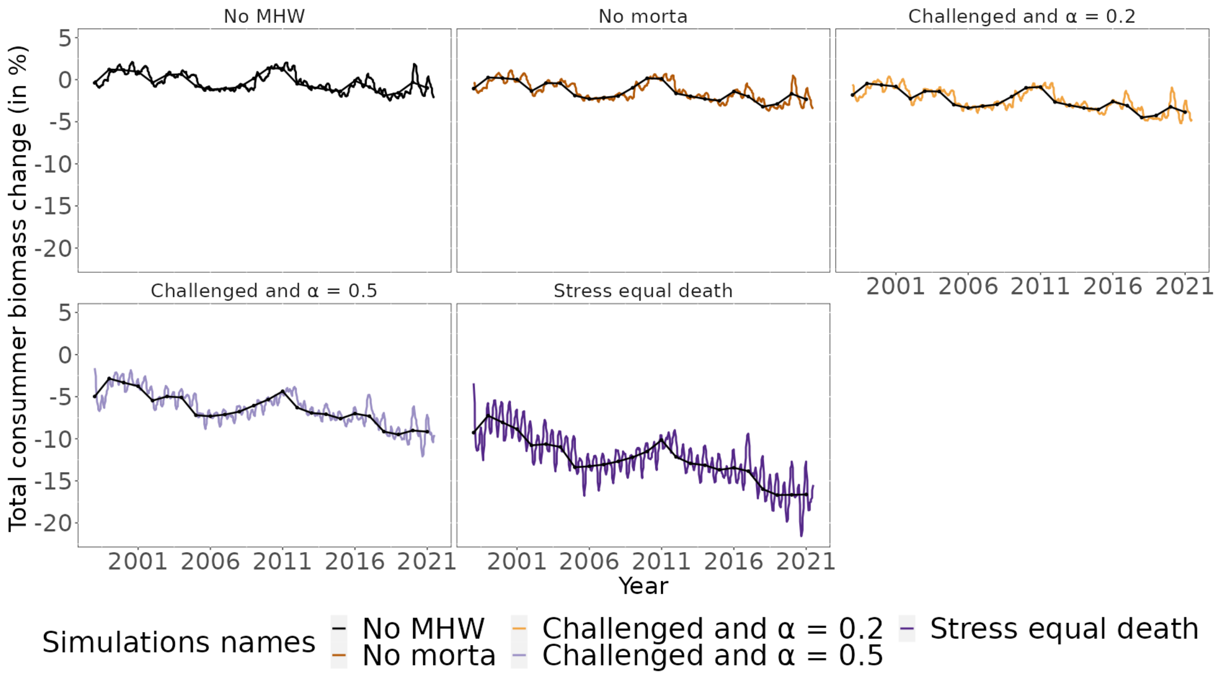

Figure S7: Yearly vs fortnight biomass evolution. With coloured lines and black lines corresponding to the fortnight and yearly biomass evolution respectively.

S6: MHWs effects on low trophic level (TL∈ [2;3[).

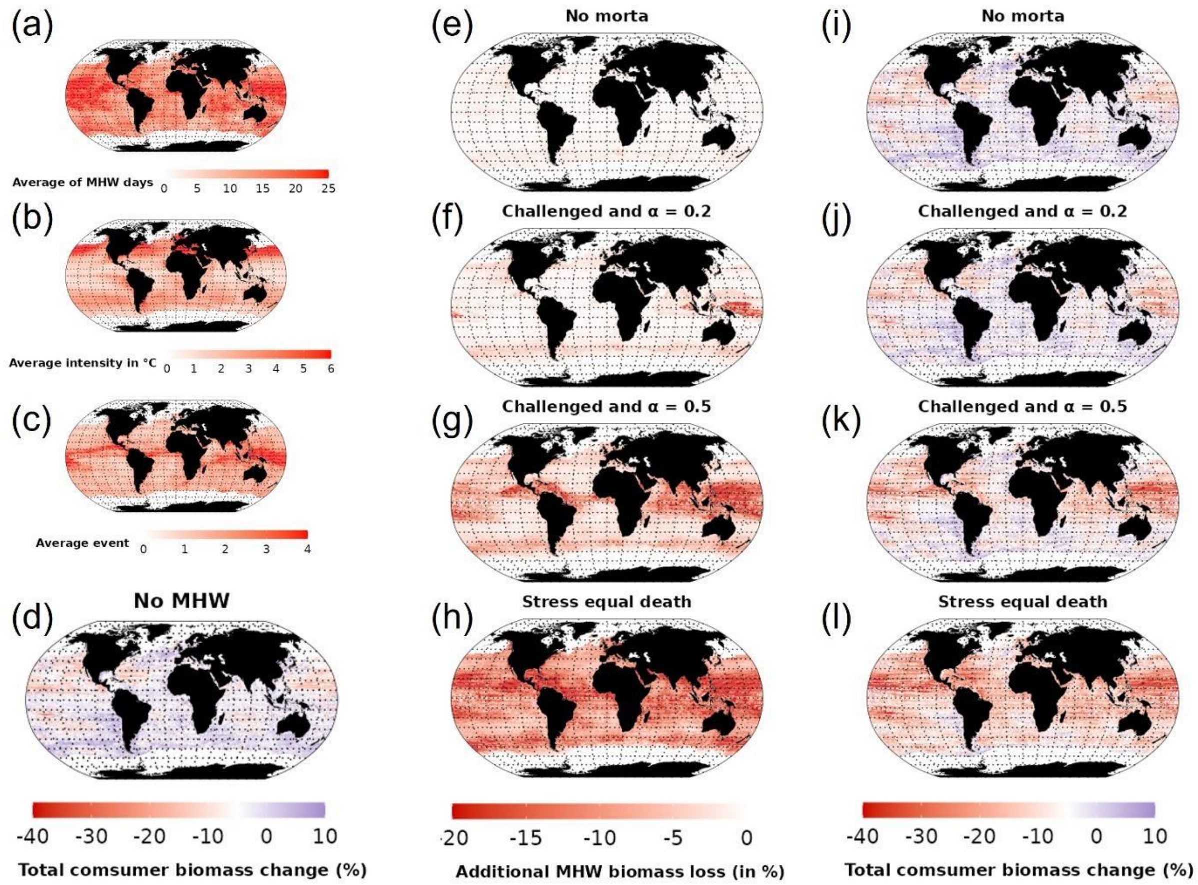

Figure S8: Additional MHW’s associated biomass loss for low TL between 2015 to 2021 compared to 1998_2009. With (a, b, and c) maps of average MHWs days, average MHWs intensity, and average number of MHWs events between 2015 and 2021, respectively; (d) average low TL (TL between 2 and 3) biomass change between 2015 and 2021 compared to 1998 to 2009 without accounting for MHWs; ((e), (f), (g), and (h)) additional low TL biomass loss associated to MHWs without additional mortality, challenged α=0.2, challenged α=0.5, and Stress equal death, respectively; ((i), (j), (k), and (l)) corresponding of the low TL biomass change between 2015 and 2021 of these simulation compare to 1998 to 2009 of No MHWs reference simulation.

S7: MHWs effects on medium trophic level (TL∈ [3;4[).

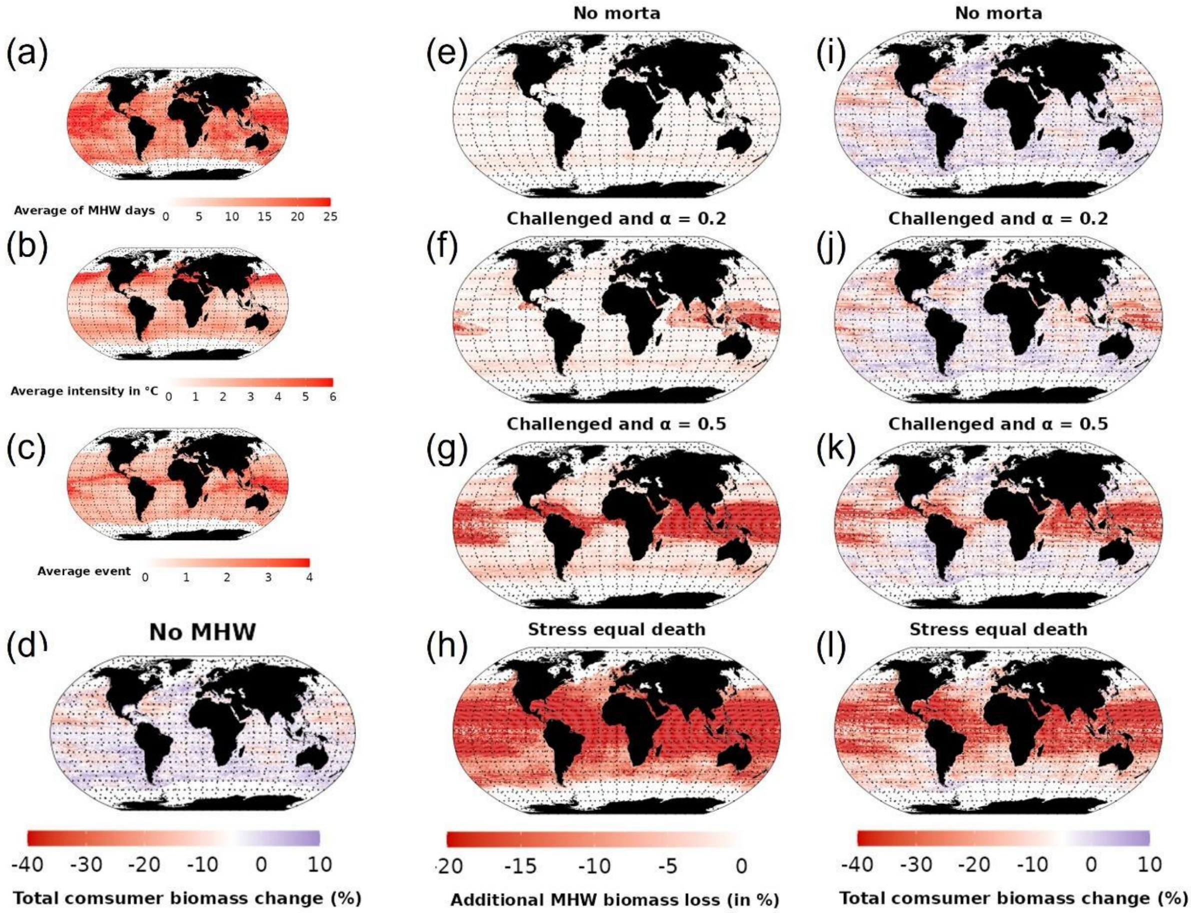

Figure S9: Additional MHW's associated biomass loss for medium TL between 2015 to 2021 compared to 1998_2009. With (a, b, and c) maps of average MHWs days, average MHWs intensity, and average number of MHWs events between 2015 and 2021, respectively; (d) average high TL (TL above 4) biomass change between 2015 and 2021 compared to 1998 to 2009 without accounting for MHWs; ((e), (f), (g), and (h)) additional high TL biomass loss associated to MHWs without additional mortality, challenged α=0.2, challenged α=0.5, and Stress equal death, respectively; ((i), (j), (k), and (l)) corresponding of the high TL biomass change between 2015 and 2021 of these simulation compare to 1998 to 2009 of No MHWs reference simulation.

S8: MHWs effects on high trophic level (TL= 4-5.5).

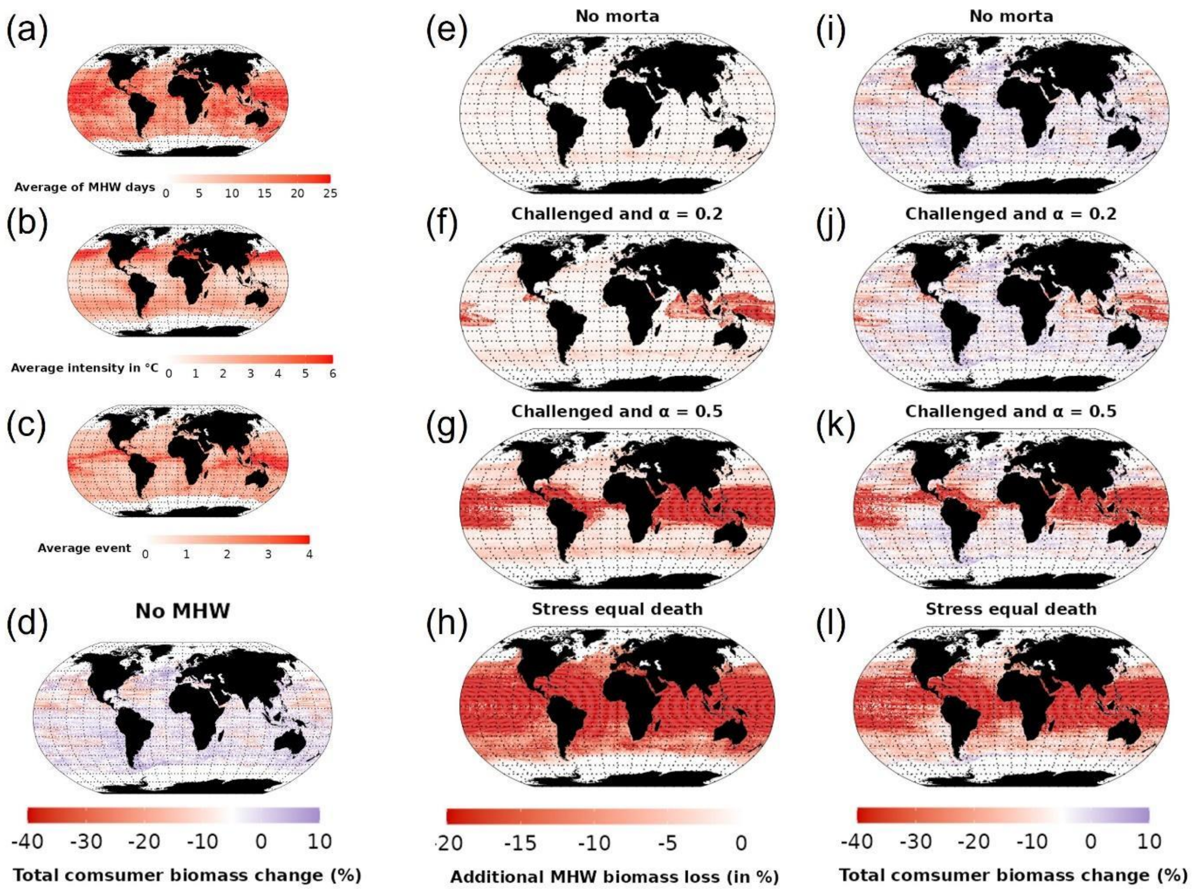

Figure S10: Additional MHW's associated biomass loss for high TL between 2015 to 2021 compared to 1998_2009. With (a, b, and c) maps of average MHWs days, average MHWs intensity, and average number of MHWs events between 2015 and 2021, respectively; (d) average medium TL (TL between 3 and 4) biomass change between 2015 and 2021 compared to 1998 to 2009 without accounting for MHWs; ((e), (f), (g), and (h)) additional medium TL biomass loss associated to MHWs without additional mortality, challenged α=0.2, challenged α=0.5, and Stress equal death, respectively; ((i), (j), (k), and (l)) corresponding of the medium TL biomass change between 2015 and 2021 of these simulation compare to 1998 to 2009 of No MHWs reference simulation.

S9: Food-web response to ‘the Blob’ MHW.

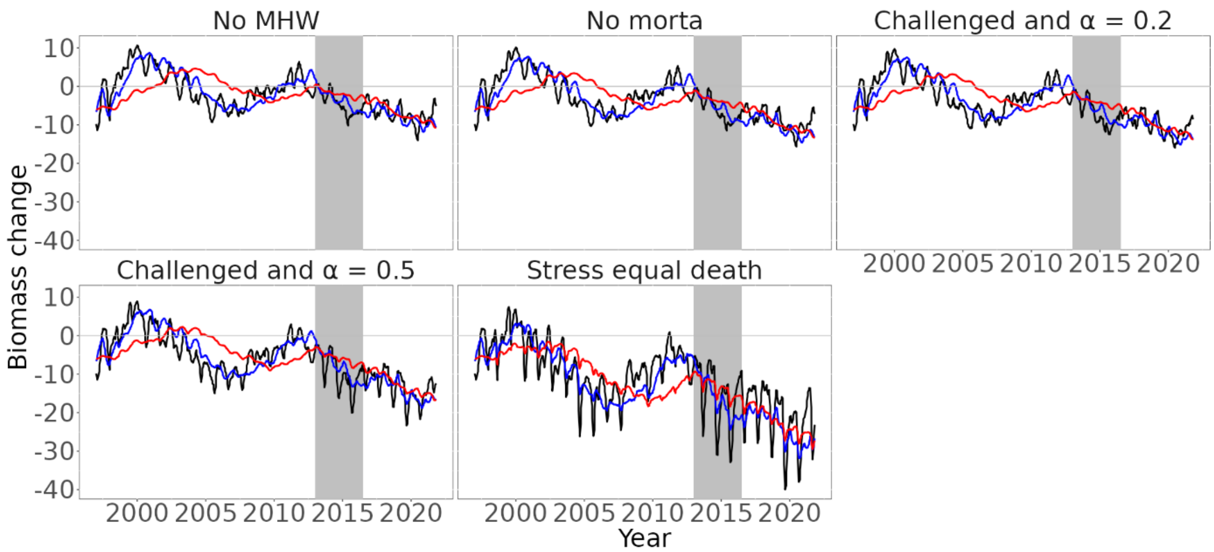

Figure S11: Blob-associated biomass loss over food web compartment compared to “without MHW” simulation 1998_2009 reference period. With low TL (trophic level $\in [2;3[$), medium TL (trophic level $\in [3;4[$), and high TL (trophic level ≥ 4) responses to MHWs corresponding to black, blue, and red lines, respectively.

S10: Biomass flow response to ‘the Blob’ MHW.

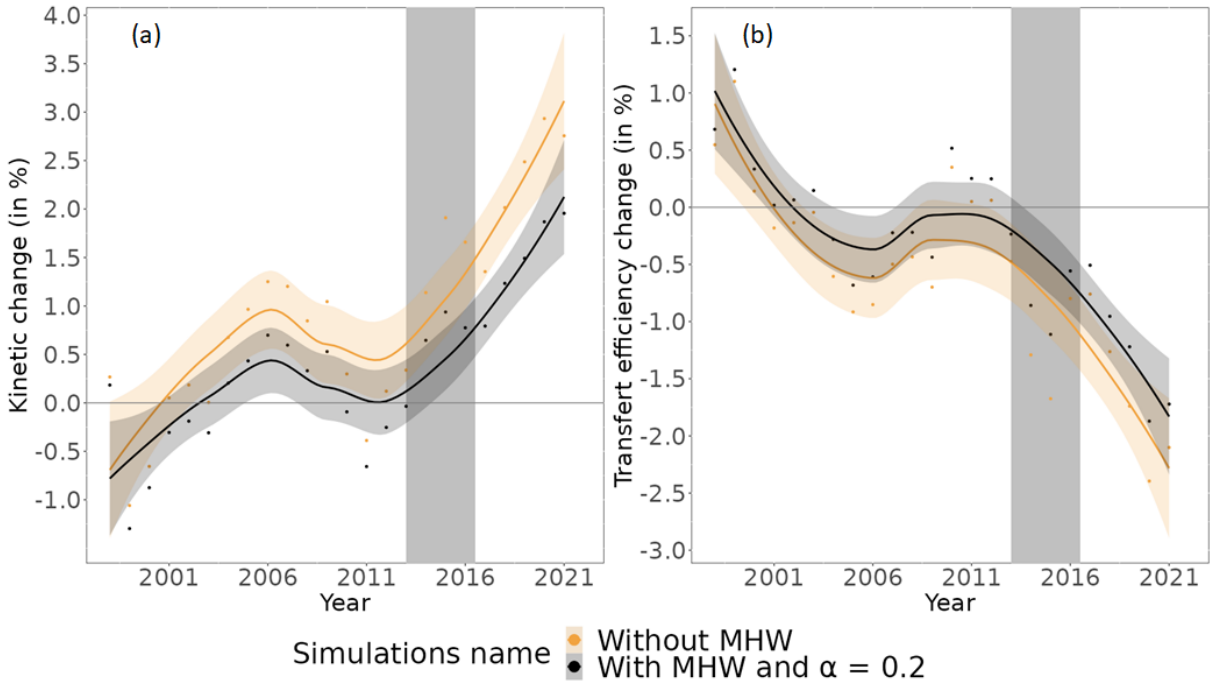

Figure S12: Hindcast changes in biomass flow processes (i.e. trophodynamic parameters) in the Northeast Pacific between 1998 and 2021 relative to 1998-2009 “Without MHW” reference. (a) Changes in flow kinetic. (b) transfer efficiency changes. The shaded areas around the curves represent the standard error. Without MHW and with MHWs scenarios correspond to the black and light orange colour